Astronomy Lab

C) Transit Observation of Exoplanets

Supervisor: Markus Mugrauer
Last Update: April 2026

1 Introduction

Since the mid-1990s, in addition to the eight planets in our solar system, planets have been discovered orbiting stars far beyond our own solar system. Since these planets do not belong to our solar system but revolve around their own host stars, they are also referred to as extrasolar planets or exoplanets for short.

To date, more than 6000 such exoplanets have been discovered using various detection methods. In addition to stars where only one exoplanet has been discovered so far, planetary systems have also been found in which several planets orbit their host star. Furthermore, exoplanets were also found in multiple star systems.

With 10-meter class telescopes, exoplanets can today even be observed directly next to their host stars, using special observation techniques such as adaptive optics and coronography in the infrared spectral range. Since planets cool down over time and thus become less luminous, they can only be observed directly around relatively young stars (a few million years old). In recent years, gas planets with several Jupiter masses (M_{Jup}) in orbits beyond about 10 au[1] have been directly imaged in this way around young stars.

In addition to the direct observation of exoplanets, most of the exoplanets known today have been detected indirectly through a precise analysis of the properties of the light emitted by their host star.

1.1 Detection Methods for Exoplanets

1.1.1 Radial Velocity Method

An important method for detecting exoplanets is based on measuring the radial velocity $v_{radial}(t)$ of the host stars, i.e., the velocity component of the stars that is oriented toward Earth (radial direction).
If a star moves toward or away from the observer, a blue or red shift occurs in the spectral lines of the star's spectrum. If the change in wavelength $\Delta\lambda = \lambda - \lambda_0$ of a spectral line relative to its rest wavelength λ_0, measured in the laboratory is known, the radial velocity of the star can be determined using the Doppler effect.

$v_{radial} \approx c \cdot \frac{\Delta\lambda}{\lambda_0}$, where c is the vacuum speed of light.

State of the art high-resolution spectrographs can detect changes in the radial velocity of stars with an accuracy better than 1 m/s. To achieve this high precision, a long-term stable reference system is required, against which the shift of the spectral lines can then be measured. For this purpose, gas absorption cells (e.g., iodine cells) or light sources (e.g., Th-Ar lamps) are used in the spectrographs to imprint a constant absorption or emission line spectrum on the spectrum of the observed stars, which then serves as a reference for measuring the wavelengths of the spectral lines.

[1] au: astronomical unit, $1\,\mathrm{au} = 1.5 \cdot 10^{11}$ m

Since the barycenter S of the planetary system always remains at rest, the star and its planet move around this point in the same orbital period P (see the left graph in Fig. 1).

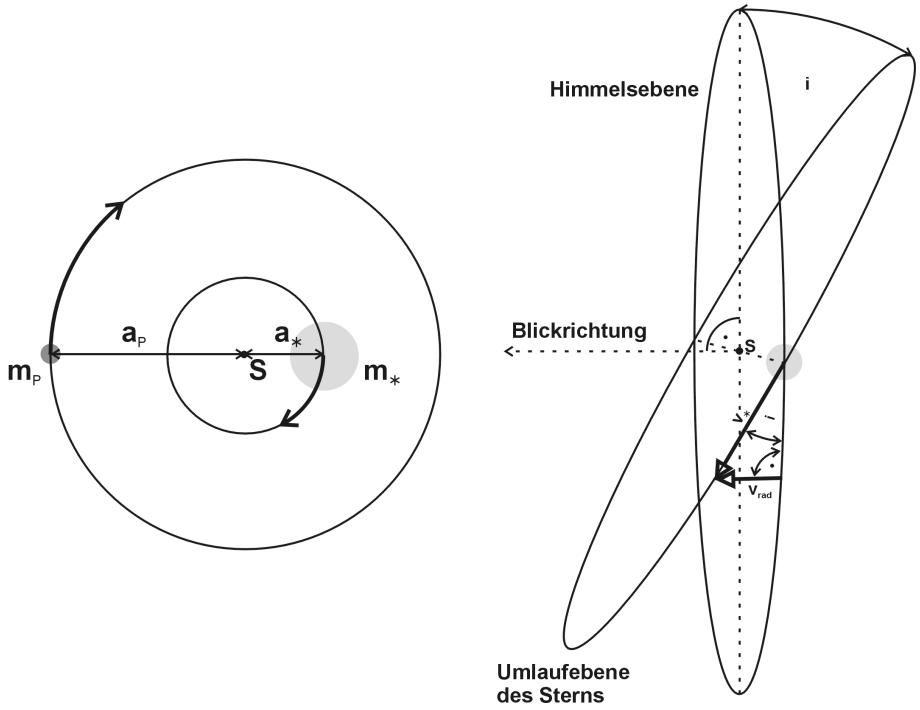

Figure 1: *Left:* Motion of the exoplanet and its host star around the barycenter S. *Right:* The position of the planet's orbit relative to the celestial plane.

The center of gravity theorem is defined by: $m_\star \cdot a_\star = m_P \cdot a_P$,

where $m_\star$ and m_P are the masses of the star and the planet, and $a_\star$ and a_P are the semi-major axes of their orbits around the barycenter.

The semi-major axis of the planetary system $a = a_\star + a_P$ is calculated using the orbital period P and the total mass of the system $M = m_\star + m_P$ from Kepler's third law:

$$a = \left(\frac{P^2 \cdot M \cdot G}{4 \cdot \pi^2}\right)^{1/3}$$

Since the mass of the host star is much greater than the mass of the exoplanet, the following approximations result: $M = m_\star + m_P \approx m_\star$, and $a = a_\star + a_P \approx a_P$ using the center of mass theorem.

This yields for the speed of the star in its orbit around the barycenter:

$$v_\star = \frac{2\pi \cdot a_\star}{P} \approx m_P \cdot \frac{2\pi \cdot a}{P \cdot m_\star}$$

As can be seen in the graph on the right in Fig. 1, the maximum observable radial velocity of the star is given by:

$v_{rad} = v_\star \cdot \sin(i)$, where i is the inclination of the planetary system.

During one orbit of the star around the barycenter, its radial velocity $v_{radial}(t)$ oscillates with amplitude v_{rad}. In the general case of an elliptical orbit, $v_{radial}(t)$ is a periodic function with amplitude v_{rad}, whose shape also depends on the eccentricity e of the planetary orbit and the argument of periastron (angle on the orbit between the ascending node[2] and the periastron). In the simpler case of a circular orbit, the following applies:

$v_{radial}(t) = v_{rad} \cdot \sin(\frac{2\pi}{P} \cdot t)$

Thanks to the Doppler effect, spectroscopic measurements can be used to determine the temporal variation of the star's radial velocity $v_{radial}(t)$ (see Fig. 2). The amplitude v_{rad} of the radial velocity curve yields the so-called minimum mass $m_P \cdot \sin(i)$ of the exoplanet:

$$m_P \cdot \sin(i) = v_{rad} \cdot \left(\frac{P \cdot m_\star^2}{2\pi \cdot G}\right)^{1/3}$$

The minimum mass of an exoplanet corresponds to the true planetary mass m_P only when the orbital inclination $i = 90°$, i.e., only when viewed exactly from the side of the planetary system. For smaller inclinations i, the true mass of the exoplanet is larger than the minimum mass determined spectroscopically.

Question:
a) Calculate the maximum amplitude v_{rad} of the radial velocity (in m/s) of a sun-like[3] star which is revolved by a Jupiter-like[4] planet or an Earth-like[5] planet on a circular orbit.
b) How large would v_{rad} be if the planets orbited the star with a period of only 4 days? What conclusions can you draw from this about the detectability of exoplanets using the radial velocity method?

Question: By what factor is the mass of an exoplanet detected by the radial velocity method underestimated on average? To determine this, calculate the expected value for $\sin(i)$, assuming that all possible orientations of the planet's orbit have equal probability.

1.1.2 Transit Method

If the orbital plane of the exoplanet is almost perpendicular to the celestial plane ($i \approx 90°$), it passes in front of its host star once per orbit when viewed from Earth. This results in the star being covered by its exoplanet, an event also known as an occultation or transit. Strictly speaking, there are actually

[2] The ascending node is the intersection of the star's orbit with the celestial plane at which the star moves away from the observer, i.e., ascends into the sky.
[3] Sun: $m_\star = 1\,M_\odot = 1.99 \cdot 10^{30}\,\mathrm{kg}$
[4] Jupiter: $m_P = 1\,M_{Jup} \approx 0.001\,M_\odot$, $a_P = 5.2\,\mathrm{au}$
[5] Earth: $m_P = 1/318\,M_{\mathrm{Jup}}$, $a_P = 1\,\mathrm{au}$

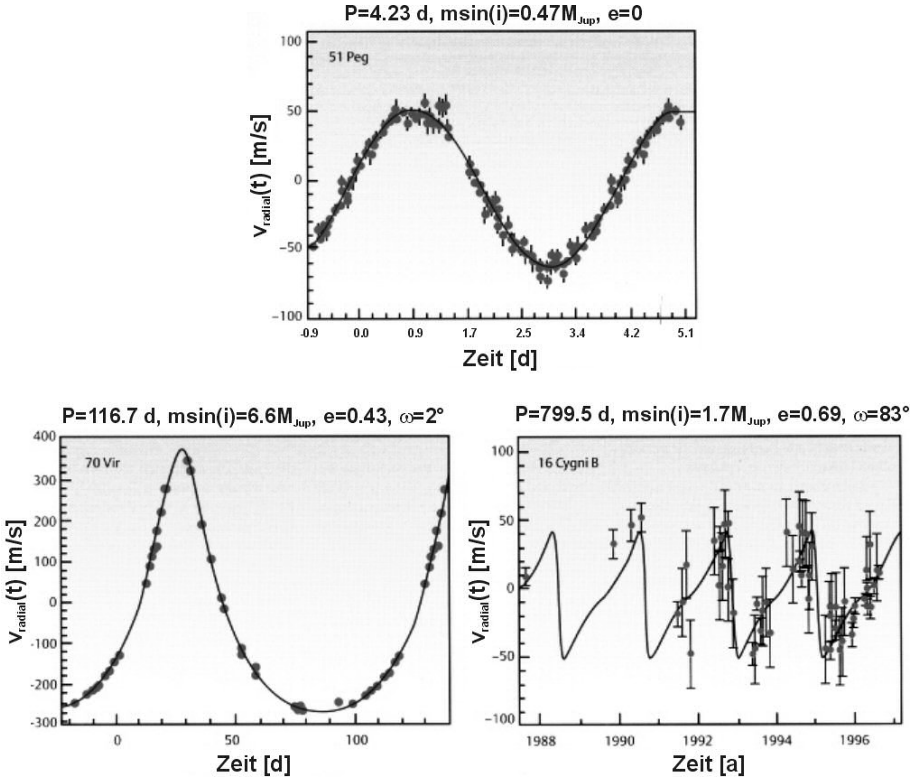

Figure 2: Radial velocity curves of the exoplanet host stars 51 Peg (top), 70 Vir (bottom left), and 16 Cyg B (bottom right). The orbit of the exoplanet 51 Peg b is circular, while the planets of 70 Vir and 16 Cyg B orbit their host stars on elliptical orbits with different arguments of periastron.

two transits, a primary transit and a secondary transit. During the primary transit, the exoplanet covers a small part of the surface of its host star as seen from Earth. Half an orbital period later, the planet disappears behind its host star as seen from Earth, and a secondary transit occurs. Important properties of an exoplanet can be deduced from the observation of primary and secondary transits. The depth D_{Prim} of the observed primary transit is given by the ratio of the radiation fluxes during F_{Prim} and outside the transit F_0, which corresponds to the ratio of the star surface still visible during the transit to the total visible star surface:

$$D_{Prim} = \frac{F_{Prim}}{F_0} = \frac{A_\star - A_P}{A_\star} = 1 - (\frac{R_P}{R_\star})^2$$

where R_P is the radius of the exoplanet and $R_\star$ is the radius of its host star.

The transit depth D_{Prim} is usually measured as the dip in brightness Δm_{Prim} in a light curve, as shown in Fig. 4:

$$\Delta m_{Prim} = -2.5 \cdot log(D_{Prim}) = -2.5 \cdot log\left(1 - (\frac{R_P}{R_\star})^2\right)$$

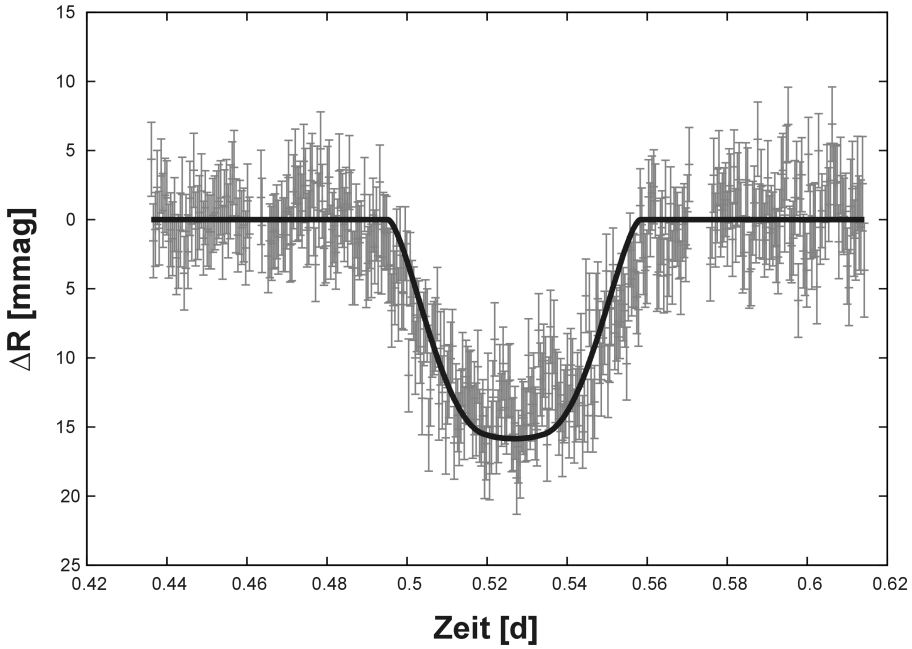

Figure 3: The light curve of the planet's host star Tres-2 at the time of the primary transit of its exoplanet Tres-2b, recorded at the University Observatory Jena with the Schmidt Telescope Camera (STK) in the V-band. The black line shows a calculated light curve that was fitted to the photometric measurements. Important properties of the exoplanet can be derived from the measurement of the depth and duration of the planetary transit.

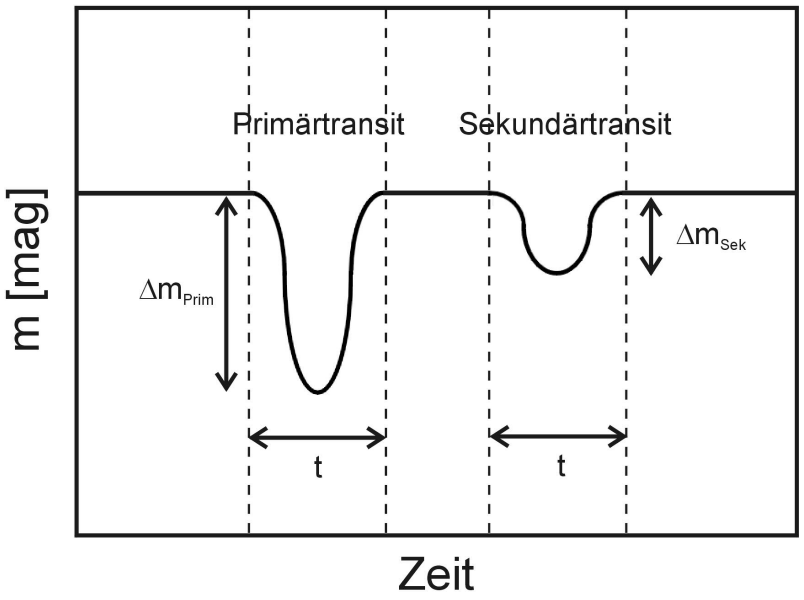

Figure 4: Theoretical light curve of a planetary transit.

If the radius of the star is known, the radius of the exoplanet can be determined using the measured dip in brightness during the primary transit Δm_{Prim}.

The primary transit of an exoplanet can already be observed in the optical spectral range, as this is where the host star has its maximum brightness. Since the exoplanet has a significantly lower surface temperature than its host star, it shines particularly brightly in the near to mid-infrared, which enables observation of the secondary transit in this wavelength range.

During the secondary transit, only the star is visible from Earth, while outside the transit, the total radiation from the star and exoplanet reaches the observer. The depth of the secondary transit D_{Sek} therefore corresponds to the ratio of the radiation flux[6] of the star $F_\star$ to the total radiation flux, i.e., the sum of the radiation flux of the star $F_\star$ and the exoplanet F_P. The depth of the secondary transit is measured as a brightness dip Δm_{sec} in a light curve, as shown in Fig. 4:

$$\Delta m_{Sek} = -2.5 \cdot log(D_{Sek}) = -2.5 \cdot log\left(\frac{F_\star}{F_\star + F_P}\right) = -2.5 \cdot log\left(\frac{R_\star^2 \cdot T_{\mathrm{eff}_\star}^4}{R_\star^2 \cdot T_{\mathrm{eff}_\star}^4 + R_P^2 \cdot T_{\mathrm{eff}_\mathrm{P}}^4}\right)$$

with $T_{\mathrm{eff}_\star}$ and $T_{\mathrm{eff}_\mathrm{P}}$ being the effective temperatures of the star and exoplanet.

If the radii of the host star $R_\star$ and its exoplanet R_P are known, as well as the effective temperature of the star $T_{\mathrm{eff}_\star}$, the effective temperature of the exoplanet $T_{\mathrm{eff}_\mathrm{P}}$ can be determined from the measured depth of the secondary transit. Measuring the depth of the secondary transit at different wavelengths yields the rough spectral distribution of the exoplanet's radiation flux $F_P(\lambda)$, which enables spectrophotometric analysis of the planet's atmosphere.

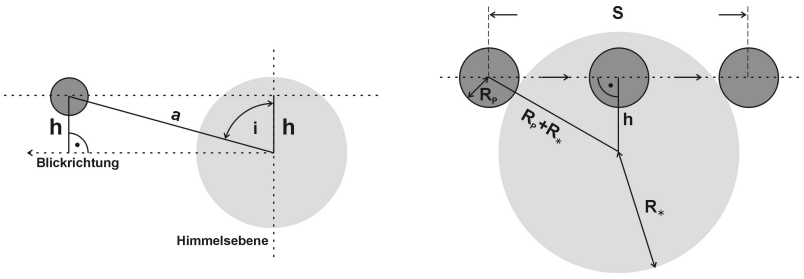

Figure 5: The geometry of planetary transit.

In addition to the depth Δm of a planetary transit, the measured light curve can also be used to determine its duration t, i.e., the length of time during which the planet is in front of the star (in the primary transit) or is covered by its host star (in the secondary transit). The two graphs in Fig. 2 illustrate the geometry of the primary transit of an exoplanet orbiting its host star in a circular orbit with a semi-major axis a and an orbital inclination i.

[6] For the total radiation flux arriving at Earth from a source at a distance d, the following applies: $F = \frac{4\pi \cdot R^2 \cdot \sigma \cdot T_{\mathrm{eff}}^4}{4\pi \cdot d^2} = \frac{R^2}{d^2} \cdot \sigma \cdot T_{\mathrm{eff}}^4$ with the radius R and the effective temperature T_{eff} of the source and the Stefan-Boltzmann constant $\sigma = 5.67 \cdot 10^{-8}\ \frac{W}{m^2 K^4}$.

Viewed from Earth (see left graphic in Fig. 2), the exoplanet passes at an altitude h above the equator of the star's disk, and the following applies: $h = a \cdot \cos(i)$

The so-called impact parameter b is often given as an auxiliary variable, which is defined as the ratio between the height h and the star radius $R_\star$:

$b = \frac{h}{R_\star} = \frac{a \cdot \cos(i)}{R_\star}$

As illustrated in the right-hand graph in Fig. 5, the transit lasts until the exoplanet has travelled the distance S:

$t = \frac{S}{v_P}$, where $v_P = \frac{2\pi \cdot a}{P}$ is the orbital velocity of the exoplanet.

The distance S is calculated as follows: $S = 2 \cdot \sqrt{(R_P + R_\star)^2 - h^2}$

and the transit duration is therefore: $t = \sqrt{(R_P + R_\star)^2 - a^2 \cdot \cos^2(i)} \cdot \frac{P}{\pi a}$

The radius R_P and the inclination i of the orbital plane of an exoplanet can be determined by measuring the depth and duration of its primary transit. If the minimum mass of the exoplanet $m_P \cdot \sin(i)$ is also known from radial velocity measurements, its true mass m_P can be determined.

The mass m_P and radius R_P of the exoplanet can be used to calculate its density:

$\rho_P = \frac{3 \cdot m_P}{4 \cdot \pi \cdot R_P^3}$

If the internal structure $\rho_P(r)$ of a planet is known, its mass can be represented as a function of the planet's radius $m_P(R_P)$ in a mass-radius diagram, as shown in Fig. 6 for different planets with different internal structures.

Question: You are observing the primary transit of an exoplanet orbiting a sun-like star ($M_\star = 1\,M_\odot$, $R_\star = 1\,R_\odot = 700000\,\mathrm{km}$) with an orbital period $P = 2\,\mathrm{d}$. In the light curve, you measure the depth and duration of the transit to be: $\Delta m_{Prim} = 0.01\,\mathrm{mag} = 10\,\mathrm{mmag}$ and $t = 102\,\mathrm{min}$. Calculate the ratio of the planet's radius to the star's radius $R_P/R_\star$, the inclination i of the planet's orbit, and the impact parameter b.

Question: A star with radius $R_\star$ is orbited by a planet (radius R_P) in a circular orbit with semi-major axis a. Derive the probability Ψ with which the transit of the exoplanet can be observed from Earth. Assume that all possible orientations of the planetary orbit are equally probable. Describe Ψ as a function of a, $R_\star$ and R_P. What conclusions can you draw about the detectability of exoplanets using the transit method?

Question: Plot the planets in our solar system: Earth ($m = 0.003\,M_\mathrm{Jup}$, $R = 0.089\,R_\mathrm{Jup}$), Jupiter, Saturn ($m = 0.3\,M_\mathrm{Jup}$, $R = 0.84\,R_\mathrm{Jup}$), and Neptune ($m = 0.054\,M_\mathrm{Jup}$, $R = 0.34\,R_\mathrm{Jup}$) into the mass-radius diagram in Fig. 6. What conclusions can you draw about the internal structure of these planets from their position in the mass-radius diagram?

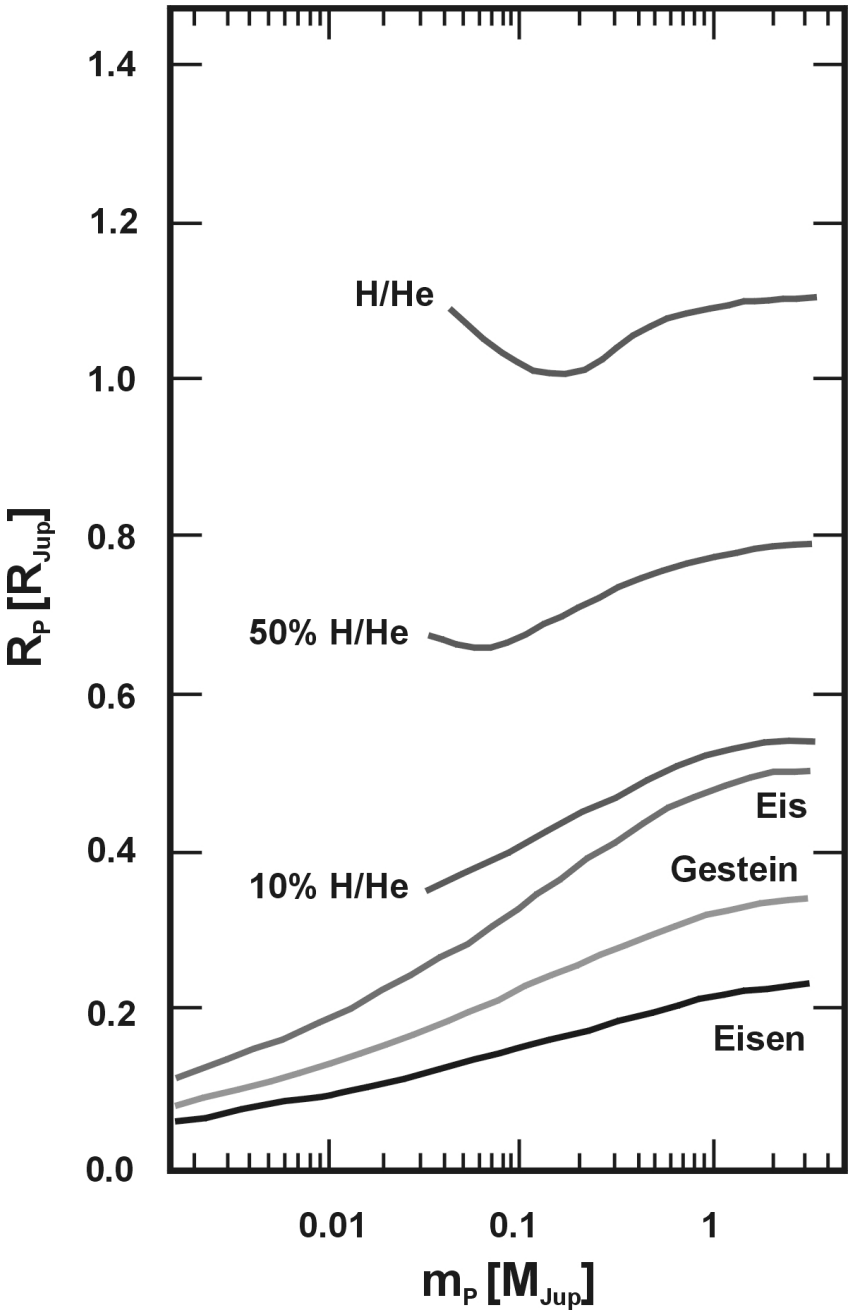

Figure 6: The mass-radius diagram together with mass-radius plots for planets of different internal compositions. The top three curves show the mass-radius plots for cool ($T < 120\,\mathrm{K}$) gas planets with a gas content of 10%, 50%, and 100% relative to their total mass. The three lower curves show the mass-radius relationships for planets composed of pure iron, rock, and ice, respectively.

1.2 CCD Detectors

Astronomical observations in the optical spectral range are nowadays mainly carried out using CCD[7] detectors. These highly light-sensitive imaging sensors consist of thousands of light sensitive elements (pixels), measuring just a few μm in size, which are arranged in a matrix. Each of these pixels in a CCD sensor is made of the semiconductor silicon, in which incident photons generate so-called electron-hole pairs. In this process, electrons are raised from the valence band of the semiconductor to the conduction band[8], leaving a hole (missing electron) in the valence band. Each pixel of the CCD detector consists of several so-called metal-oxide-semiconductor (MOS) contacts. When a voltage is applied to a MOS contact, a potential well forms in the band structure of the semiconductor at the interface between the oxide and the semiconductor, into which the charge carriers generated in the pixel during exposure then migrate and are collected. During the detector readout process, the voltages at the individual MOS contacts of the pixels are varied. The charge carriers stored in a pixel are thus shifted vertically from one pixel in a pixel row to the corresponding pixel in the adjacent pixel row until they reach the output register at the edge of the CCD sensor, a covered and therefore light-insensitive pixel row. In the output register, the charge carriers are then shifted horizontally from pixel to pixel and finally reach the readout amplifier integrated on the CCD detector. There, the charge quantity of each individual pixel is amplified and then measured in a downstream external readout electronics via a capacitance (voltage drop) and finally digitized by means of an A/D converter (see Fig. 7). The measurement error that occurs during amplification, charge measurement, and digitization is also referred to as readout noise RN.

The number of electrons N_e generated in a pixel during an exposure is directly proportional to the number of incident photons N_γ over a wide dynamic range. The following applies for every wavelength:

$N_e(\lambda) = QE(\lambda) \cdot N_\gamma(\lambda)$, where QE is the CCD quantum efficiency.

The quantum efficiency of modern CCD detectors reaches maximum values of over 90%. These image sensors are therefore extremely light-sensitive and can detect almost all photons that strike them.

Thermally activated electron-hole pairs also occur in the semiconductor, generating the so-called dark current I_{Dark} of a CCD detector, which increases exponentially with rising temperature. The signal generated by the dark current during exposure must be subtracted from each light image[9], which was recorded with the CCD detector. This is achieved by taking a dark image[10], using the same exposure time as the corresponding light image.

[7] CCD: *Charge Coupled Device*

[8] When an electron in the semiconductor transitions from the valence band to the conduction band, the so-called band gap energy E_{gap} must be overcome. For silicon, $E_{\mathrm{gap}} = 1.12\,\mathrm{eV}$

[9] Light image: Exposure of the CCD detector with the camera shutter open.

[10] Dark image: Exposure of the CCD detector with the camera shutter closed.

Subtracting the dark image from the light image ultimately provides the image information that was generated only by the photons on the CCD sensor.

In addition to dark frame subtraction, the varying sensitivity of individual pixels must also be corrected. For this purpose, a so-called flatfield image[11] is taken. The different sensitivity of the individual pixels is achieved by dividing a light image freed from dark current by the flatfield image. Dark frame subtraction, followed by flatfield division, is also referred to as data reduction, whereby the following applies to each reduced CCD image:

$$reduced\ \ image(t_1) = \frac{rawimage(t_1) - darkimage(t_1)}{\langle flatfieldimage(t2) - darkimage(t2) \rangle_{normalized}}$$

where t_1 and t_2 are the exposure times of the raw image and the flatfield image, respectively.

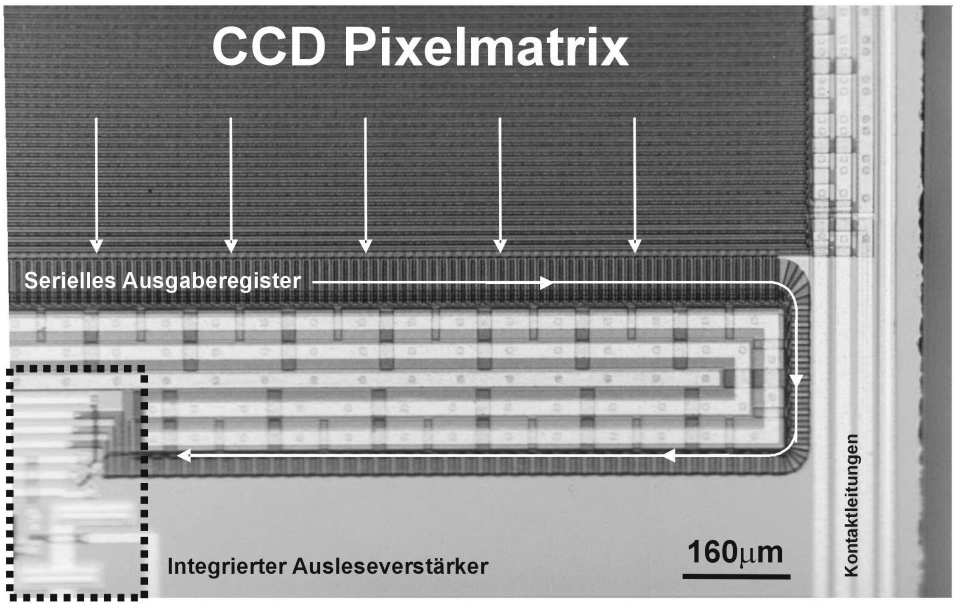

Figure 7: Detailed view of a CCD detector. The white arrows indicate the direction of movement of the charge carriers during the readout process.

Question: At what minimum wavelength λ_{Limit} do you expect a quantum efficiency $QE = 0$ for a CCD detector?

Question: Why do CCD detectors have to be cooled during operation?

Question: Calculate the typical noise N of a CCD detector with the exposure time t, the dark current I_{Dark} and the readout noise RN.

[11] Flatfield image: Image of a uniformly illuminated surface (e.g., white wall in the dome of the observatory or the sky during twilight).

1.3 Photometry

The measurement of the brightness of celestial objects is also referred to as photometry in astronomy. Photometric measurements are often performed using various color filters that only allow photons of a precisely defined wavelength range to pass through, which are then detected by an imaging sensor. The apparent brightness of a celestial object m_{Filter} measured in a filter is defined as:

$$m_{\text{Filter}} = -2.5 \cdot log(F_{\text{Filter}}) + C_{\text{Filter}}$$

where F_{Filter} is the radiation flux of the object measured through the filter and C_{Filter} is the filter constant. The apparent brightness is given in the unit mag (magnitude), whereby, according to the above definition, a larger magnitude value corresponds to a lower radiation flux. The difference in brightness between two celestial objects with radiation fluxes F_1 and F_2 is therefore:

$$\Delta m = m_1 - m_2 = -2.5 \cdot log\left(\frac{F_1}{F_2}\right)$$

CCD detectors enable precise measurement of the apparent brightness of celestial objects. In what is known as aperture photometry, the radiation flux of an object is measured on the CCD detector within a circular area (aperture). The aperture is typically selected to be 3 to 5 times larger than the full width at half maximum (FWHM) of the source to be measured. This ensures that the entire flux of the source is captured in the aperture. The radiation flux of the background is then measured in a circular ring (annulus) around the aperture. The difference between the measured aperture and background flux gives the instrumental magnitude m_{inst} of the object:

$$m_{\text{inst}} = -2.5 \log(F_{\text{Aperture}} - F_{\text{Background}})$$

The apparent brightness m of an object can be calculated from its measured instrumental magnitude:

$$m = m_{\text{inst}} + z$$

If the apparent brightness m of a reference object is known in an image, the constant z can be determined by measuring the instrumental magnitude m_{inst} of the object. This then allows the apparent brightness of all objects detected in the image to be determined.

1.4 University Observatory Jena

All data processed in this experiment was recorded at the University Observatory Jena. The observatory is located approximately 10 km west of Jena in a grove near the small village of Großschwabhausen. Three telescopes are operated in the observatory dome, installed on a fork mount. The mount carries a reflector telescope with a main mirror diameter of $D = 90\,\text{cm}$, to whose tube two further smaller telescopes are attached, a 25 cm Cassegrain and a Fraunhofer refractor with a 20 cm objective diameter. All telescopes are equipped with modern CCD cameras. All images processed and analyzed in this experiment were taken with the Cassegrain-Teleskop-Kamera (CTK) operated at the 25 cm Cassegrain telescope of the observatory. The individual characteristics of the CTK are summarized in the article[12] *CTK - A new CCD Camera at the University Observatory Jena - Mugrauer M. (2009, AN 330, 419).*

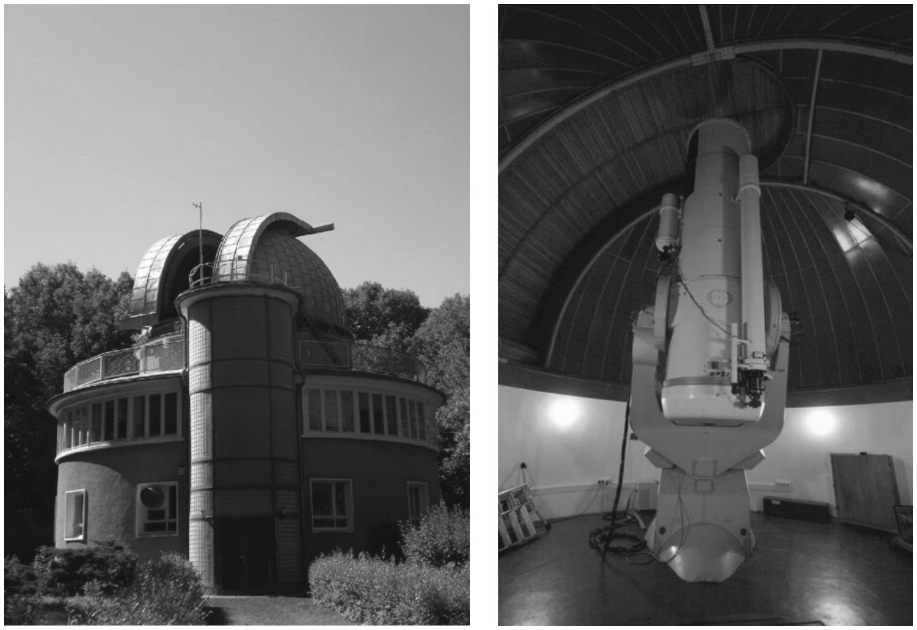

Figure 8: *Links:* The building of the University Observatory Jena with its dome open in the grove near Großschwabhausen (ca. 10 km west of Jena). *Right:* View inside the dome of the University Observatory Jena. This photo shows the 90 cm reflector telescope on its parallactic fork mount together with the 25 cm Cassegrain (left) and the 20 cm Fraunhofer refractor (right), both of which are mounted on the tube of the 90 cm reflector telescope. Three CCD cameras (STK, CTK, RTK) and a fiber-optic-coupled Échelle spectrograph (FLECHAS) are used for astronomical research at the observatory.

[12] Available online at: `http://arxiv.org/PS_cache/arxiv/pdf/0903/0903.4116v1.pdf`

2 Experiment Procedure

As part of this experiment, imaging data of the planet host star GSH1 is being analyzed, which was taken at the University Observatory Jena with the CTK in the I-band. The star is orbited by an exoplanet whose transit is observable from Earth. The available CTK imaging data was recorded exactly at the time of the exoplanet's transit. The known properties of the parent star GSH1 and its planet are summarized in Table Tab. 1 in the appendix. A finding chart is available for identifying the star in the CTK images, which is shown in Fig. 10 in the appendix. In addition, weather permitting, a planetary transit will be observed at the University Observatory Jena. The properties of the exoplanet can then be derived from the light curve obtained.

2.1 Determination of the apparent brightness of stars

In the first part of this experiment, the apparent brightness of stars in the vicinity of the planet host star GSH1 will be determined using aperture photometry. The photometric measurements are performed using the program. Start *ESO-MIDAS* in the *Linux* terminal by entering the command:

inmidas

The CTK data for the planet host star GSH1 are located in the directory *gsh1*. To access them, change to the directory *GSH1* in the *Linux* terminal:

cd gsh1

Now get an overview of all the data in this directory by entering the command:

ls *

Now load the CTK raw image of the star GSH1 into the image memory by entering the command:

load/image gsh1_80s.fits s=3 c=f,ihap

The CTK image is now displayed in the *MIDAS* display. The displayed images can also be saved as ps files if desired. To do this, enter:

copy/display POSTSCRIPT

The ps file created in this way is always saved under the file name *screen01.ps* and can be renamed using the *mv* command, e.g.:

mv screen01.ps rawimage.ps

To reduce the individual CTK raw images, a dark image (*dark_80s.fits*) with the same exposure time as the raw images and a flatfield image (*flat.fits*) are stored in the directory *gsh1*.

Load the dark image and the flatfield image into the image memory one after the other and save both images as ps files (for later display in the report). Briefly describe the individual detector-specific artifacts that you can see on the raw, dark, and flatfield images and explain how they are caused.

Now reduce the CTK raw image (*gsh1_80s.fits*). To do this, first remove the background signal generated by the dark current in the raw image by subtracting the dark image. Enter the following command:

comp bild_darksub = gsh1_80s.fits - dark_80s.fits

In the next step the different sensitivity of the individual pixels must be corrected by dividing them by the flatfield image. To do this, enter:

comp bildred = bild_darksub / flat.fits

Now load the reduced image *bildred.bdf* into the image memory and create a copy of the *MIDAS* display in ps format. Compare the reduced image with the raw image and briefly describe the most striking differences between the two images.

Figure 9 shows the section of the sky around the planet host star GSH1. Within an angular distance of $2'$ around GSH1, there are 6 other fainter stars (a-f) whose apparent I-band magnitudes are to be determined using aperture photometry. To do this, first measure the instrumental magnitudes m_{inst} of the stars by entering the command:

mag/circ ? ? A,B,C

where A is the diameter of the aperture, B is the distance between the aperture and the annulus, and C is the thickness of the annulus in pixels. After entering the command, the selected aperture and annulus appear in the *MIDAS* display. Now move the cross in the center of the aperture to all stars whose instrumental magnitude is to be measured and then click the left mouse button. The instrumental magnitudes and measurement errors of the stars are displayed in the *Linux* terminal in the columns *magnitude* and *mag-sigma*. Clicking the right mouse button ends the photometric measurement[13].

Note: The aperture diameter must be selected so that the entire detected flux of a star lies completely within the aperture. The distance between the aperture and the annulus should not be too large. If possible, there should be no sources in the annulus during the measurement.

Now calculate the brightness difference (with measurement error) between stars a-f and the planet's parent star GSH1. Using the known apparent I-band brightness of GSH1 ($m_I = 11.60 \pm 0.01$ mag), the apparent brightness of stars a-f in the I-band (with their measurement errors) can be determined. Plot the achieved photometric measurement accuracy of all stars against their apparent brightness

[13] All apertures can be removed from the *MIDAS* display with the command: **cl/ch o**

in a diagram. How can the distribution of the measured values in the diagram be explained?

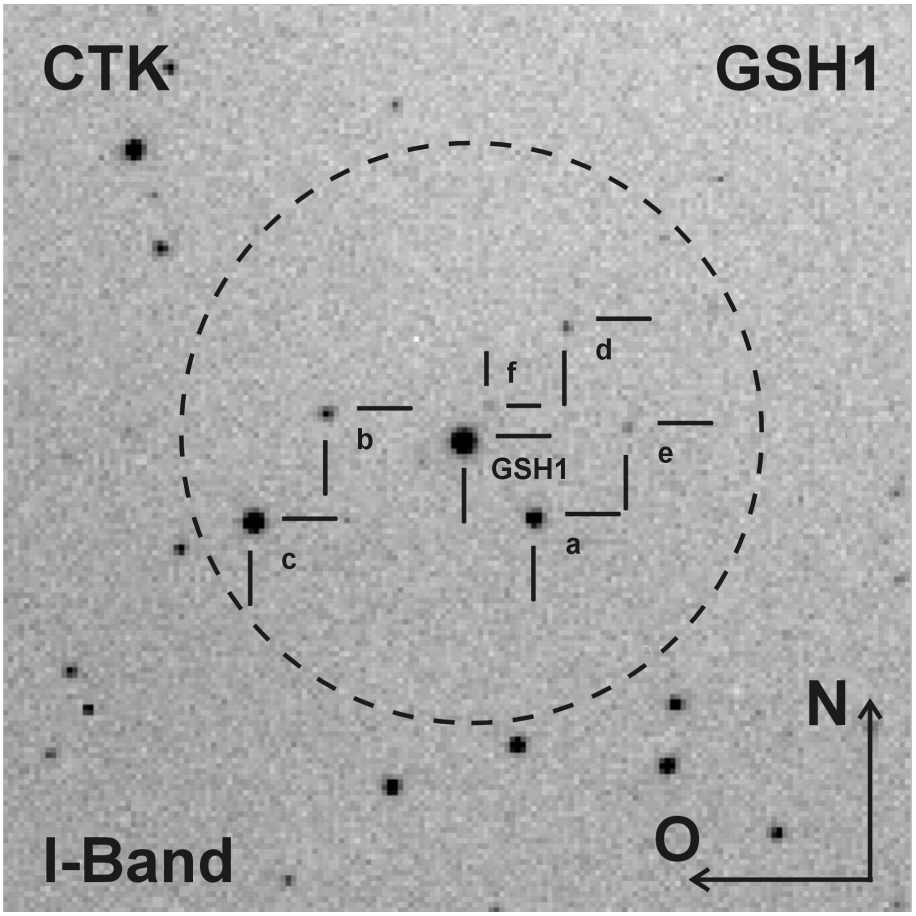

Figure 9: The planet host star GSH1 imaged with the CTK in the I-band. The positions of the star and its nearest neighbors within an angular distance of $2'$ (dashed circle) are marked. North is at the top and east is on the left.

2.2 Transit observation of exoplanets

In the second part of this experiment, the transit light curve of the planet host star GSH1 will be obtained from the available observation data. The properties of the exoplanet GSH1 b can then be determined from the light curve.

The reduction of the CTK data and the subsequent photometric analysis are performed using the *Windows* software *MuniWin*.

Start *MuniWin* by entering the command:

muniwin

A summary of the most important *MuniWin* commands can be found in the appendix in Fig. 11.

First, load all CTK images of the planet host star GSH1 into the working memory. To do this, click on the *Add files* icon (or alternatively use the keyboard shortcut *Ctrl-O*) and select all CTK images of the star. Confirm your image selection by clicking on the *Add* button. Then close the working window again by clicking on the *Close* button. All selected image files are now listed in the *File Name* column in the *MuniWin* main window.

Next, the important image information (e.g., recording time, exposure time, filter, etc.) is read from the individual image files. To do this, click on the *Convert files* icon and select the *all files in project* option on the workspace. Now start the image information import process by clicking on the *OK* icon. If the image information for an image file has been successfully imported, this is indicated by a green check mark to the left of the image name in the *File Name* column.

Now it's time to reduce the CTK images, starting with dark frame subtraction. To do this, click on the *Dark-frame correction* icon and select the appropriate dark frame. Then start the dark frame subtraction by clicking on the *OK* button. If the dark frame subtraction was successful, this is indicated by a black *D* to the left of the image name in the *File Name* column. Next comes the flatfield division. To do this, click on the *Flat-frame correction* icon. Select the flatfield image and start the flatfield division by clicking on the *OK* button. If the flatfield division was successful, this is indicated by a black *F* to the left of the image name in the *File Name* column.

The next step is to use aperture photometry to measure the instrumental magnitudes of the stars detected in the individual CTK images. To do this, click on the *Photometry* icon and then select *all files in project* on the workspace. Start the photometric measurement by clicking on the *OK* button. *MuniWin* now determines the instrumental brightness of all detected stars in each image for different aperture sizes. In addition, the sky brightness, the instrumental brightness of the detection limit, and the mean value of the half-value width of all detected stars are measured in each image. The corresponding Julian date[14] JD is then calculated from the recording time of each image.

Next, identify the stars in each frame for which instrumental magnitudes could be measured in all images. To do this, click on the *Match stars* icon and select the image in which the most stars were detected as the reference frame (*reference frame*) on the workspace. Confirm your entry by clicking on the *OK* button. The number of stars detected in each image is displayed on the right side of the workspace in the *Stars* column. If the matching process (*star matching*) was successful, this is indicated by a green left-right arrow to the left of the image name in the *File Name* column.

Now click on the *Find variables* area and then on the *Var* icon in the newly opened workspace. Identify the planet host star in the image displayed using

[14] JD: Time span in days calculated from 1 January 4713 BC at 12:00 UT.

the finding chart in the appendix. Then move the mouse to the planet host star in the image and select the star by clicking the left mouse button. The star will be marked as a red dot labelled *var* in the image. The upper left diagram shows the photometric measurement accuracy of all detected stars plotted against their instrumental magnitude. The position of the planet host star is represented by a red dot in this diagram. The lower diagram shows the light curve of the star for the currently selected comparison star (marked in the image as a green dot labelled *comp*). The standard deviation *stdev* (in mag) of the photometric measurements relative to their mean value is displayed to the right of the light curve. The standard deviation of the measured values is largely determined by the variability of the selected comparison star. Well-suited comparison stars show low variability and should also have a similar brightness to the planet host star. To select a comparison star, click on the *Comp* area. Now you can select the star either in the image or directly in the *stdev*-mag diagram. The pixel coordinates and the registration number of the comparison star are displayed to the right of the light curve. Now identify two comparison stars that are as suitable as possible and note down their coordinates and registration numbers. Then close the workspace by clicking on the *Close* button. Save the current star selection.

Now click on the *Choose stars* icon and mark the selected comparison stars in the image. Confirm your selection by clicking on the *OK* button. The light curve of the planet host star, relative to the selected comparison stars, is now displayed. The standard deviation of the measured values from the mean value must now be minimized by adjusting the aperture size. To do this, remove the black check mark to the right of *Default aperture* and select the aperture size that achieves the smallest standard deviation (*Std. dev.*). Click on the *Save data* field to save the light curve generated for the parent star and name it *GSH1.txt*. Then close the workspace by clicking on the *Close* button.

All image data imported into *MuniWin* can be deleted from the working memory by clicking on the *Clear files* icon.

Now load the light curve file *GSH1.txt* using the *Kate* editor. To do this, go to the directory where you saved the file in the console and then enter *kate GSH1.txt* in the console. Remove all data points without a measured value (99.9999) from the file and save the edited file.

Before modelling the planetary transit, any linear brightness trend that may be present in the light curve must be removed. The script *Detrending.xls* is available on the desktop for this purpose. Open the script by clicking on it and load the file *GSH1.txt* (*Open* $\rightarrow$ *File* and, if necessary, select the options *Space & Merge delimiters* under *Separator Options*). Copy the columns for date JD and brightness $V-C$ from the file *GSH1.txt* to columns A & B of the script and then remove the unnecessary rows at the bottom of the script in columns H & I. Double-click on the plot on the right to determine the data points that cover the time period outside the transit, and then copy these values into columns D & E. Finally, copy the data from the detrended light curve in columns H & I into a new text file, entering the formatting of the original light curve file (JD $V-C$) in the first line.

Make sure that JD and $V - C$ are specified with five decimal places.

The detrended light curve is modelled using the *AstroImageJ* program. Start the program in the console by entering the command aij. Activate the MultiPlot Tool (fifth icon from the right in the control bar). To load the light curve, click on *File* in the *Multi-Plot Main* menu and then select the file of the detrended light curve in the *Open Table from File* menu item. In the *Multi-plot Y-data* menu, select the columns for JD and $V - C$ in the detrended light curve file under *X-data* and *Y-data*. Then read the times for the beginning and end of the transit from the displayed plot of the light curve and enter them in the *Multi-plot Main* menu at the top under *V. Marker 1* and *V. Marker 2*. To define the time range outside the transit, click on the *Copy* icon at the bottom of the *Fit and Normalize Region Selection* area. The light curve fitted to the data points is displayed in the diagram. Save the diagram as a PDF copy by pressing the *PDF* button. The values for the transit depth (*Depth*) and transit duration *t14* can be found in the Fit menu. For the fit errors, take one-fifth of the RMS value of the fit for the depth and twice the average time interval of the individual measured values for the duration.
Now use the determined values for the depth and duration of the planetary transit to calculate the radius (in R_{Jup}), orbital inclination i, true mass (in M_{Jup}), and density (in ρ_{Jup}) of the exoplanet GSH1 b. The script *Transitfitting.xls* is available on the desktop for this purpose. Then plot the exoplanet in the mass-radius diagram in Fig. 6. How can the position of the exoplanet in this diagram be explained? (Hint: Also calculate the equilibrium temperature (in K) of the exoplanet.)

Perform the same analysis for the planetary transit that you have observed yourself at the University Observatory Jena.

A Appendix

Table 1: Properties of the star GSH1 and its exoplanet GSH1 b.

GSH1	
Spectral Type	G6V
$T_{\mathrm{eff}_\star}$	$5720 \pm 150\,\mathrm{K}$
$m_\star$	$0.92 \pm 0.04\,M_\odot$
$R_\star$	$0.81 \pm 0.03\,R_\odot$

GSH1 b	
P	$1.3062 \pm 0.0001\,\mathrm{d}$
$m_P \cdot \sin(i)$	$1.91 \pm 0.08\,M_{\mathrm{Jup}}$

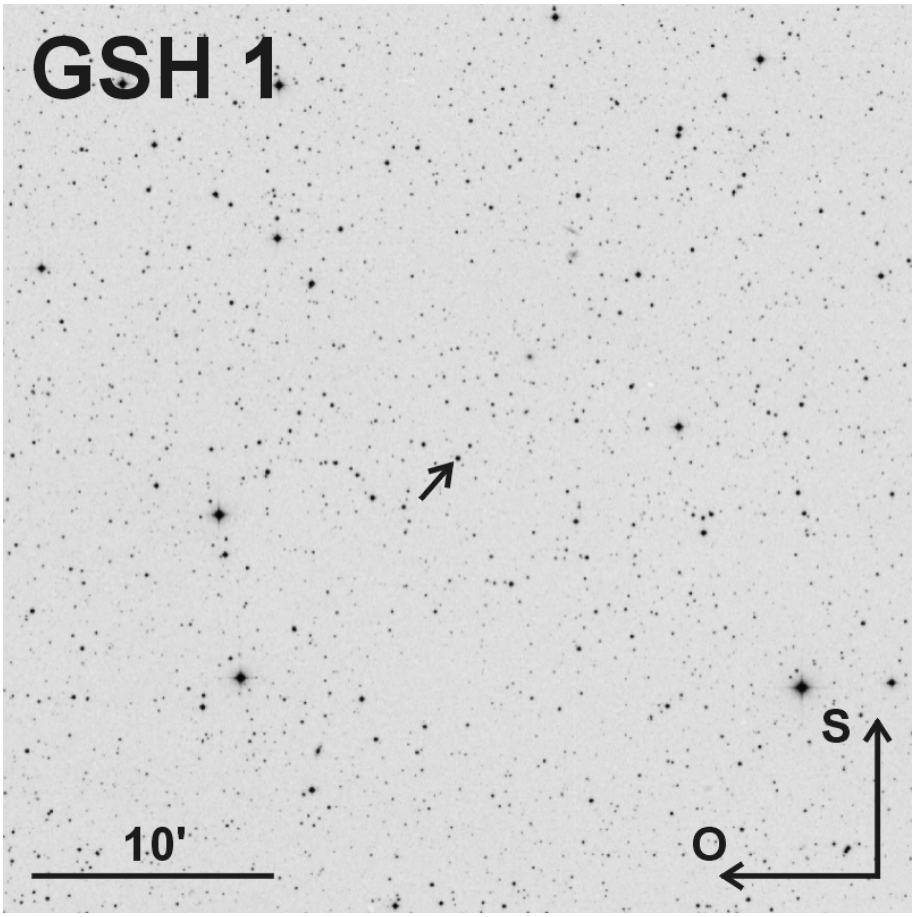

Figure 10: The finding chart for the planet host star GSH1. The section of the sky shown measures $37.7' \times 37.7'$, which corresponds to the CTK field of view. South is at the top, east is on the left. The host star GSH1 is marked with a black arrow.

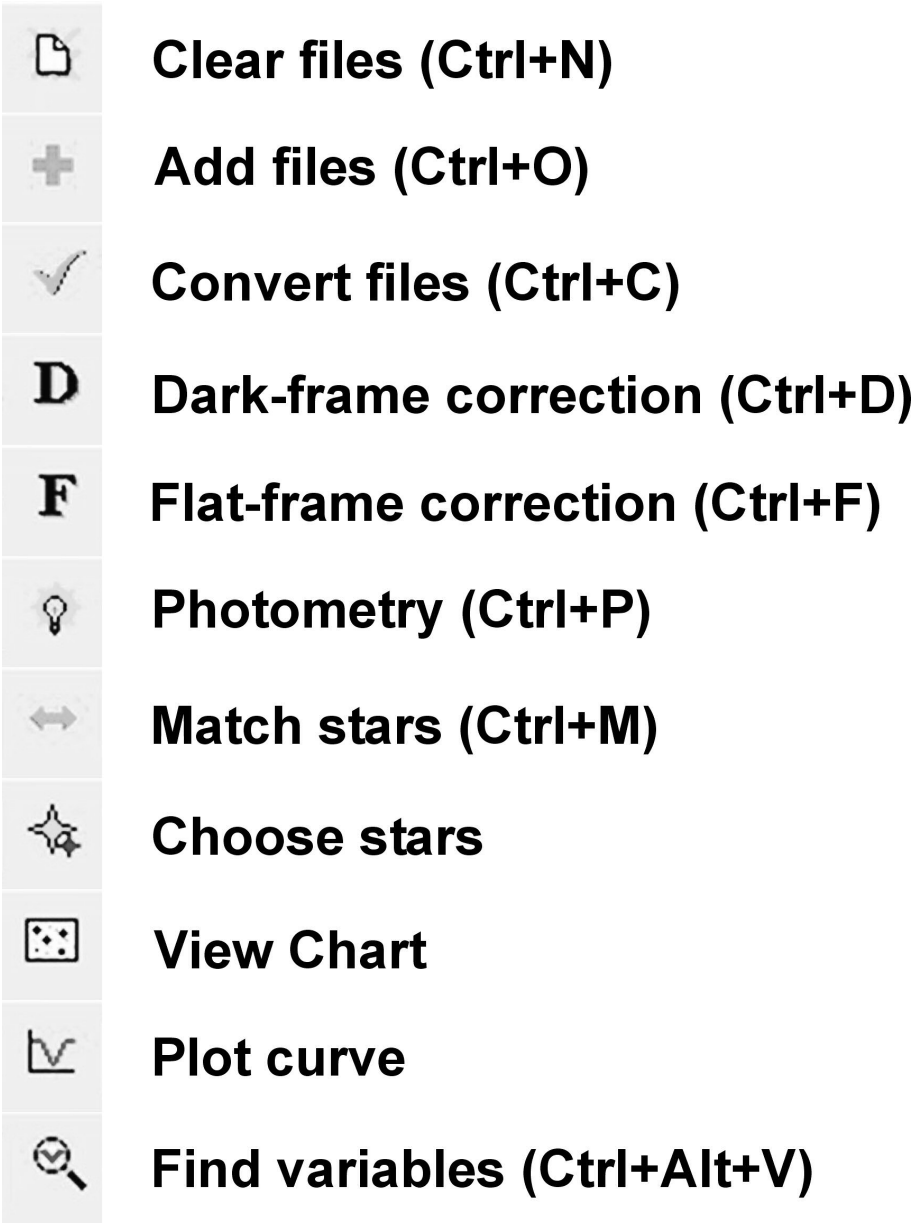

Figure 11: Summary of the individual *MuniWin* commands.